Frequency Response Data-based Multiple Peak Filter Design Applied to High-Precision Stage in Translation and Pitching

Masahiro Mae, Wataru Ohnishi and Hiroshi Fujimoto
The University of Tokyo
5-1-5, Kashiwanoha, Kashiwa, Chiba, Japan
mmae@ieee.org, ohnishi@ieee.org, fujimoto@k.u-tokyo.ac.jp

Koichi Sakata
Nikon Corporation
471, Nagaodaicho, Sakae, Yokohama, Kanagawa, Japan
koichi.sakata@nikon.com

Abstract—Tuning of feedback controllers in high-precision stages needs a lot of time and skills. In particular, multiple filter design for multi-input multi-output systems is difficult because of a large number of controller parameters in each axis and a coupling problem between each axis. In this study, the frequency response data-based multiple peak filter design method is proposed to reduce the error. The multiple peak filters are designed by convex optimization with the objective function to reduce the error. The effectiveness of the proposed method is validated in the simulated data of the two-degree-of-freedom high-precision stage in translation and pitching.

Index Terms—Concave-convex procedure, Data-based design, Frequency responses, Disturbance rejection, Peak filter, MIMO system

I. INTRODUCTION

Disturbance rejection is important in the high-precision stages with the scan motion. It improves the tracking performance of the high-precision scan stage used in the industry such as manufacturing semiconductors and flat panel displays (FPD) [1]. Many high-precision stages in the industry have multi-degree-of-freedoms (multi-DOFs) such as moving with translation and pitching in each axis and are multi-input multi-output (MIMO) systems. They are typically controlled with 2-DOF control with a feedforward controller for reference tracking and a feedback controller for disturbance rejection [2]. The model-based feedforward controller design approach for the MIMO system with translation and pitching is proposed [3]. However, a feedback controller design for disturbance rejection in MIMO systems has several challenges that it is time-consuming and needs experience because of the interaction between each axis and many controller tuning parameters.

To design without the heuristic tuning approach depending on experiences, several approaches of the frequency response data-based feedback controller design with convex optimization are proposed such as using the concave-convex procedure [4]. In the data-based design approach, the structure of the controller is important for the physical interpretation and effort of on-site control engineers.

The disturbance can be rejected by the peak filter with the same resonance frequency [5] because of the internal model principle [6] and, auto-tuning method for one peak filter is proposed [7]. However, the multiple peak filter design using convex optimization has not been reported yet. The convex optimization has the challenge to formulate the controller in affine to avoid multiplying the tuning parameters each other. In this study, the frequency response data-based multiple peak filter design method using convex optimization is presented.

The main contributions of this study are i) the structured multiple peak filter is formulated, ii) the peak filter is directly designed with frequency response data, and iii) the control problem can be solved with convex optimization.

The outline of this paper is as follows. In Section II, the control problem is formulated. The frequency response data-based multiple peak filter design is presented in Section III. The advantages of the approach are demonstrated in Section IV. Conclusions are presented in Section V.

II. PROBLEM FORMULATION

A. Controlled system

The controlled system is given as a frequency response data of n_u-input n_y-output open-loop system $\boldsymbol{G}(\mathrm{j}\omega_{k_f}) \in \mathbb{C}^{n_y \times n_u}$ as follows:

$$\boldsymbol{G}(\mathrm{j}\omega_{k_f}) = G_{(k_y, k_u)}(\mathrm{j}\omega_{k_f}), \tag{1}$$

where the indices of inputs, outputs, and frequency response data are $k_u = 1, \dots, n_u$, $k_y = 1, \dots, n_y$, and $k_f = 1, \dots, n_f$. In this study, the square system ($n_u = n_y$) is considered.

B. Designed controller

The n_y-input n_y-output diagonal peak filter $\boldsymbol{F}(\mathrm{j}\omega_{k_f}, \boldsymbol{\rho})$ is designed as follows:

$$\boldsymbol{F}(\mathrm{j}\omega_{k_f}, \boldsymbol{\rho}) = \mathrm{diag}(F_{k_y}(\mathrm{j}\omega_{k_f}, \boldsymbol{\rho}_{k_y})), \tag{2}$$

where the tuning parameter is $\boldsymbol{\rho} = [\boldsymbol{\rho}_1, \dots, \boldsymbol{\rho}_{n_y}]$.

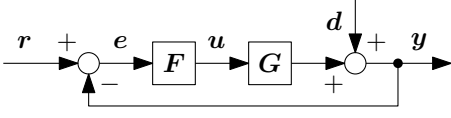Fig. 1. Block diagram of the controlled system. The given open-loop system $\boldsymbol{G}$ is controlled by the designed diagonal peak filter $\boldsymbol{F}$. $\boldsymbol{r}$, $\boldsymbol{e}$, $\boldsymbol{u}$, $\boldsymbol{y}$, and $\boldsymbol{d}$ denote reference, error, input, output, and disturbance, respectively. The objective is to minimize the error $\boldsymbol{e}$.

The designed peak filter in each output is given by

$$
\begin{aligned}
&F_{k_y}(\mathrm{j}\omega_{k_f}, \boldsymbol{\rho}_{k_y}) \\
&= 1 + \sum_{k_p=1}^{n_{p,k_y}} \frac{\rho_{k_y,(k_p,2)}(\mathrm{j}\omega_{k_f})^2 + \rho_{k_y,(k_p,1)}(\mathrm{j}\omega_{k_f})}{(\mathrm{j}\omega_{k_f})^2 + 2\zeta_{p,k_y,k_p}\omega_{p,k_y,k_p}(\mathrm{j}\omega_{k_f}) + \omega_{p,k_y,k_p}^2}
\end{aligned}
$$

$$
= \begin{bmatrix} 1 \\ \rho_{k_y,(1,1)} \\ \rho_{k_y,(1,2)} \\ \vdots \\ \rho_{k_y,(n_{p,k_y},1)} \\ \rho_{k_y,(n_{p,k_y},2)} \end{bmatrix}^{\mathsf{T}} \begin{bmatrix} 1 \\ \dfrac{(\mathrm{j}\omega_{k_f})}{(\mathrm{j}\omega_{k_f})^2 + 2\zeta_{p,k_y,1}\omega_{p,k_y,1}(\mathrm{j}\omega_{k_f}) + \omega_{p,k_y,1}^2} \\ \dfrac{(\mathrm{j}\omega_{k_f})^2}{(\mathrm{j}\omega_{k_f})^2 + 2\zeta_{p,k_y,1}\omega_{p,k_y,1}(\mathrm{j}\omega_{k_f}) + \omega_{p,k_y,1}^2} \\ \vdots \\ \dfrac{(\mathrm{j}\omega_{k_f})}{(\mathrm{j}\omega_{k_f})^2 + 2\zeta_{p,k_y,n_{p,k_y}}\omega_{p,k_y,n_{p,k_y}}(\mathrm{j}\omega_{k_f}) + \omega_{p,k_y,n_{p,k_y}}^2} \\ \dfrac{(\mathrm{j}\omega_{k_f})^2}{(\mathrm{j}\omega_{k_f})^2 + 2\zeta_{p,k_y,n_{p,k_y}}\omega_{p,k_y,n_{p,k_y}}(\mathrm{j}\omega_{k_f}) + \omega_{p,k_y,n_{p,k_y}}^2} \end{bmatrix}
$$

$$
= \boldsymbol{\rho}_{k_y}^{\mathsf{T}} \boldsymbol{\phi}_{k_y}(\mathrm{j}\omega_{k_f}), \tag{3}
$$

where the index of the peak filters in each output is $k_p = 1, \ldots, n_{p,k_y}$, the tuning parameter in each output is $\boldsymbol{\rho}_{k_y} \in \mathbb{R}^{2n_{p,k_y}+1}$, and the resonance frequency and damping coefficient of each peak filter are $\omega_{p,(k_y,k_p)}$ and $\zeta_{p,(k_y,k_p)}$.

C. Control objective

The control objective considered in this study is to minimize the error frequency spectrum of the given open-loop system $\boldsymbol{G}$ with the designed diagonal peak filter $\boldsymbol{F}$ as shown in Fig. 1.

The error frequency spectrum matrix in the open-loop system $\boldsymbol{G}(\mathrm{j}\omega_{k_f})$ is given by the experiment as follows:

$$
\boldsymbol{E}_0(\mathrm{j}\omega_{k_f}) = \begin{bmatrix} \boldsymbol{e}_{0,1}(\mathrm{j}\omega_{k_f}) & \cdots & \boldsymbol{e}_{0,n_e}(\mathrm{j}\omega_{k_f}) \end{bmatrix}, \tag{4}
$$

where the experiment is conducted in n_e times, the index of the experiment is $k_e = 1, \ldots, n_e$, and the error frequency spectrum in each experiment $\boldsymbol{e}_{0,k_e}(\mathrm{j}\omega_{k_f}) \in \mathbb{C}^{n_y \times 1}$ is given by

$$
\boldsymbol{e}_{0,k_e}(\mathrm{j}\omega_{k_f}) = \begin{bmatrix} e_{0,k_e,1}(\mathrm{j}\omega_{k_f}) & \cdots & e_{0,k_e,n_y}(\mathrm{j}\omega_{k_f}) \end{bmatrix}^{\mathsf{T}}. \tag{5}
$$

The disturbance frequency spectrum matrix is given from the error frequency spectrum matrix as follows:

$$
\boldsymbol{D}(\mathrm{j}\omega_{k_f}) = \boldsymbol{S}_0^{-1}(\mathrm{j}\omega_{k_f})\boldsymbol{E}_0(\mathrm{j}\omega_{k_f}) \tag{6}
$$

where $\boldsymbol{S}_0(\mathrm{j}\omega_{k_f}) = (\boldsymbol{I} + \boldsymbol{G}(\mathrm{j}\omega_{k_f}))^{-1} \in \mathbb{C}^{n_y \times n_y}$ is the sensitivity function matrix with the open-loop system $\boldsymbol{G}(\mathrm{j}\omega_{k_f})$ and $\boldsymbol{I} \in \mathbb{R}^{n_y \times n_y}$ is an identity matrix. The elements of the disturbance frequency spectrum matrix is given by

$$
\boldsymbol{D}(\mathrm{j}\omega_{k_f}) = \begin{bmatrix} \boldsymbol{d}_1(\mathrm{j}\omega_{k_f}) & \cdots & \boldsymbol{d}_{n_e}(\mathrm{j}\omega_{k_f}) \end{bmatrix}, \tag{7}
$$

where the disturbance frequency spectrum in each experiment $\boldsymbol{d}_{k_e}(\mathrm{j}\omega_{k_f}) \in \mathbb{C}^{n_y \times 1}$ is given by

$$
\boldsymbol{d}_{k_e}(\mathrm{j}\omega_{k_f}) = \begin{bmatrix} d_{k_e,1}(\mathrm{j}\omega_{k_f}) & \cdots & d_{k_e,n_y}(\mathrm{j}\omega_{k_f}) \end{bmatrix}^{\mathsf{T}}. \tag{8}
$$

The error frequency spectrum matrix in the open-loop system $\boldsymbol{G}(\mathrm{j}\omega_{k_f})\boldsymbol{F}(\mathrm{j}\omega_{k_f}, \boldsymbol{\rho})$ is given by the calculation with the disturbance frequency spectrum matrix as follows:

$$
\boldsymbol{E}(\mathrm{j}\omega_{k_f}, \boldsymbol{\rho}) = \boldsymbol{S}(\mathrm{j}\omega_{k_f}, \boldsymbol{\rho})\boldsymbol{D}(\mathrm{j}\omega_{k_f}), \tag{9}
$$

where $\boldsymbol{S}(\mathrm{j}\omega_{k_f}, \boldsymbol{\rho}) = (\boldsymbol{I} + \boldsymbol{G}(\mathrm{j}\omega_{k_f})\boldsymbol{F}(\mathrm{j}\omega_{k_f}, \boldsymbol{\rho}))^{-1} \in \mathbb{C}^{n_y \times n_y}$ is the sensitivity function matrix with the open-loop system $\boldsymbol{G}(\mathrm{j}\omega_{k_f})\boldsymbol{F}(\mathrm{j}\omega_{k_f}, \boldsymbol{\rho})$.

The control objective considered in this study is to minimize the error frequency spectrum $\boldsymbol{E}(\mathrm{j}\omega_{k_f}, \boldsymbol{\rho})$ with the designed diagonal peak filter $\boldsymbol{F}(\mathrm{j}\omega_{k_f}, \boldsymbol{\rho})$.

III. APPROACH

A. Objective function

The objective function is designed to minimize the error frequency spectrum matrix $\boldsymbol{E}(\mathrm{j}\omega_{k_f}, \boldsymbol{\rho})$ with the designed diagonal peak filter $\boldsymbol{F}(\mathrm{j}\omega_{k_f}, \boldsymbol{\rho})$.

From (9), the weighted error frequency spectrum matrix is given by

$$
\boldsymbol{W}^{-1}\boldsymbol{E}(\mathrm{j}\omega_{k_f}, \boldsymbol{\rho}) = \boldsymbol{W}^{-1}(\boldsymbol{I} + \boldsymbol{G}(\mathrm{j}\omega_{k_f})\boldsymbol{F}(\mathrm{j}\omega_{k_f}, \boldsymbol{\rho}))^{-1}\boldsymbol{D}(\mathrm{j}\omega_{k_f}), \tag{10}
$$

where $\boldsymbol{W} \in \mathbb{R}^{n_y \times n_y}$ is the scaling matrix of the error.

The Moore–Penrose inverse of the weighted error frequency spectrum matrix is given by

$$
(\boldsymbol{W}^{-1}\boldsymbol{E}(\mathrm{j}\omega_{k_f}, \boldsymbol{\rho}))^+ = (\boldsymbol{W}^{-1}(\boldsymbol{I} + \boldsymbol{G}(\mathrm{j}\omega_{k_f})\boldsymbol{F}(\mathrm{j}\omega_{k_f}, \boldsymbol{\rho}))^{-1}\boldsymbol{D}(\mathrm{j}\omega_{k_f})))^+, \tag{11}
$$

$$
\boldsymbol{E}^+(\mathrm{j}\omega_{k_f}, \boldsymbol{\rho})\boldsymbol{W} = \boldsymbol{D}^+(\mathrm{j}\omega_{k_f})(\boldsymbol{I} + \boldsymbol{G}(\mathrm{j}\omega_{k_f})\boldsymbol{F}(\mathrm{j}\omega_{k_f}, \boldsymbol{\rho}))\boldsymbol{W}. \tag{12}
$$

In this approach, 1-norm of each row of $\boldsymbol{E}^+(\mathrm{j}\omega_{k_f}, \boldsymbol{\rho})\boldsymbol{W}$ is evaluated in each frequency. The objective function is given by

$$
\underset{\boldsymbol{\rho}}{\text{maximize}} \quad \min_{\forall k_e, \forall k_f} \|\boldsymbol{D}_{(k_e,:)}^+(\mathrm{j}\omega_{k_f})(\boldsymbol{I} + \boldsymbol{G}(\mathrm{j}\omega_{k_f})\boldsymbol{F}(\mathrm{j}\omega_{k_f}, \boldsymbol{\rho}))\boldsymbol{W}\|_1. \tag{13}
$$

B. Constraint of sensitivity function

The robust stability condition in each output is considered with the upper bound of the gain of the sensitivity function as follows:

$$
|w_{s,k_y}(\mathrm{j}\omega_{k_f})| - |G_{(k_y,k_y)}(\mathrm{j}\omega_{k_f})F_{k_y}(\mathrm{j}\omega_{k_f}, \boldsymbol{\rho}) + 1| \leq 0, \tag{14}
$$

where $w_{s,k_y}(\mathrm{j}\omega_{k_f})$ is the weighting function of the upper bound of the gain of the sensitivity function.

The input saturation condition in each output is considered with the lower bound of the gain of the sensitivity function as follows:

$$
|w_{u,k_y}(\mathrm{j}\omega_{k_f})| - |G_{(k_y,k_y)}(\mathrm{j}\omega_{k_f})F_{k_y}(\mathrm{j}\omega_{k_f}, \boldsymbol{\rho}) + 1| \geq 0, \tag{15}
$$

where $w_{u,k_y}(\mathrm{j}\omega_{k_f})$ is the weighting function of the lower bound of the gain of the sensitivity function.

C. Optimization problem formulation

The optimization problem is formulated with the objective function and the constraints of the sensitivity function as follows.

$$\underset{\boldsymbol{\rho}}{\text{maximize}} \quad \min_{\forall k_e, \forall k_f} \| \boldsymbol{D}^+_{(k_e,:)}(\mathrm{j}\omega_{k_f})(\boldsymbol{I} + \boldsymbol{G}(\mathrm{j}\omega_{k_f})\boldsymbol{F}(\mathrm{j}\omega_{k_f}, \boldsymbol{\rho}))\boldsymbol{W} \|_1 \quad (16)$$

$$\underset{\forall k_f, \forall, k_y}{\text{subject to}} \quad |w_{s,k_y}(\mathrm{j}\omega_{k_f})| - |G_{(k_y,k_y)}(\mathrm{j}\omega_{k_f})F_{k_y}(\mathrm{j}\omega_{k_f}, \boldsymbol{\rho}) + 1| \leq 0 \quad (17)$$

$$|G_{(k_y,k_y)}(\mathrm{j}\omega_{k_f})F_{k_y}(\mathrm{j}\omega_{k_f}, \boldsymbol{\rho}) + 1| - |w_{u,k_y}(\mathrm{j}\omega_{k_f})| \leq 0 \quad (18)$$

Because of the nonlinearity objective function in (16), the optimization problem is reformulated with the linear objective function γ as follows.

$$\underset{\boldsymbol{\rho}}{\text{maximize}} \quad \gamma \quad (19)$$

$$\underset{\forall k_e, \forall k_f, \forall, k_y}{\text{subject to}} \quad \gamma - \| \boldsymbol{D}^+_{(k_e,:)}(\mathrm{j}\omega_{k_f})(\boldsymbol{I} + \boldsymbol{G}(\mathrm{j}\omega_{k_f})\boldsymbol{F}(\mathrm{j}\omega_{k_f}, \boldsymbol{\rho}))\boldsymbol{W} \|_1 \leq 0 \quad (20)$$

$$|w_{s,k_y}(\mathrm{j}\omega_{k_f})| - |G_{(k_y,k_y)}(\mathrm{j}\omega_{k_f})F_{k_y}(\mathrm{j}\omega_{k_f}, \boldsymbol{\rho}) + 1| \leq 0 \quad (21)$$

$$|G_{(k_y,k_y)}(\mathrm{j}\omega_{k_f})F_{k_y}(\mathrm{j}\omega_{k_f}, \boldsymbol{\rho}) + 1| - |w_{u,k_y}(\mathrm{j}\omega_{k_f})| \leq 0 \quad (22)$$

D. Concave-convex procedure

The constraints (20) and (21) in the optimization problem are the differences in convex functions and they are non-convex. In this approach, the concave-convex procedure [4] is applied. A sequential linearization is applied around the current solution and the new feasible sets (23) and (24) become convex subsets of the original feasible sets. The parameter is optimized by repeating the update of the optimization problem and the convex optimization calculation.

In this approach, it is not secured to converge to the global optimum solution. It is likely to converge local optimum solution or saddle point. However, the optimization problem can be solved by convex optimization with monotonous convergence secured. Therefore, the quasi-optimized solution can be derived with easy and stable calculation compared to nonlinear optimization.

IV. SIMULATION

A. Motion system

The 2-DOF motion system of a high-precision stage in the translation x and the pitching θ_y is illustrated in Fig. 2. It is noted that the number of the output is $n_y = 2$. The index $k_y = 1$ means the translation x and the index $k_y = 2$ means the pitching θ_y.

The given open-loop system $\boldsymbol{G}$ is consists of the 2-DOF motion system and the given feedback controller. The given open-loop system $\boldsymbol{G}$ is controlled by the designed diagonal peak filter $\boldsymbol{F}$ as shown in Fig. 3.

B. Conditions

The number of frequency response data points is set to $n_f = 1000$, and they are arranged at linearly even intervals in the range from $3\,\text{Hz}$ to $30\,\text{Hz}$. The frequency response data of the given open-loop system $\boldsymbol{G}$ is shown in Fig. 4.

TABLE I
PARAMETERS OF INITIAL PEAK FILTER F_x.

k_p	$\omega_{p,1,k_p}$	$\zeta_{p,1,k_p}$	$\rho_{1,k_p,1}$	$\rho_{1,k_p,2}$
1	$2\pi \times 4.78$	0.10	0.67	-4.94×10^{-03}
2	$2\pi \times 5.86$	0.10	0.61	7.41×10^{-04}
3	$2\pi \times 6.65$	0.10	2.80	2.25×10^{-02}
4	$2\pi \times 8.81$	0.10	0.92	3.99×10^{-02}

TABLE II
PARAMETERS OF INITIAL PEAK FILTER F_{θ_y}.

k_p	$\omega_{p,2,k_p}$	$\zeta_{p,2,k_p}$	$\rho_{2,k_p,1}$	$\rho_{2,k_p,2}$
1	$2\pi \times 4.78$	0.10	0.65	-6.02×10^{-03}
2	$2\pi \times 5.86$	0.10	0.27	1.78×10^{-05}
3	$2\pi \times 6.65$	0.10	0.94	7.93×10^{-03}
4	$2\pi \times 8.81$	0.10	1.13	8.26×10^{-02}

The error data is measured by pre-experiment in the constant scan velocity of the translation x with $0.5\,\text{m/s}$ for $12\,\text{times}$ ($n_e = 12$). The scaling matrix of the error is given by the mean error of all experiments at all frequencies in each output as follows:

$$\boldsymbol{W} = \text{diag}\left(\frac{1}{n_e n_f} \sum_{k_e=1}^{n_e} \sum_{k_f=1}^{n_f} |e_{0,k_e,k_y}(\mathrm{j}\omega_{k_f})| \right). \quad (25)$$

The weighting function of the upper bound of the gain of the sensitivity function is given by

$$w_{s,k_y}(\mathrm{j}\omega_{k_f}) = v_s \times \begin{cases} (1 + G_{(k_y,k_y)}(\mathrm{j}\omega_{k_f})) & (\omega_{k_f} \leq \omega_{k_y,s_{\max}}) \\ (1 + G_{(k_y,k_y)}(\mathrm{j}\omega_{k_y,s_{\max}})) & (\omega_{k_f} > \omega_{k_y,s_{\max}}) \end{cases}, \quad (26)$$

where $v_s = 1/1.01$ and

$$\min_{\forall k_f} |1 + G_{(k_y,k_y)}(\mathrm{j}\omega_{k_f})| = |1 + G_{(k_y,k_y)}(\mathrm{j}\omega_{k_y,s_{\max}})|. \quad (27)$$

The weighting function of the lower bound of the gain of the sensitivity function is given by

$$w_{u,k_y}(\mathrm{j}\omega_{k_f}) = v_u \times (1 + G_{(k_y,k_y)}(\mathrm{j}\omega_{k_f})) \quad (\omega_{k_f} \leq \omega_{k_y,s_{\max}}), \quad (28)$$

where $v_u = 3$.

The parameters of the initial peak filter is given by the heuristic approach [5] with the constraints of the sensitivity function as shown in TABLE I and TABLE II.

The iterative calculation in the optimization is continued until the improvement of the objective function is less than $1\,\%$. The optimization problem is calculated by YALMIP [8] and Mosek [9].

C. Optimization result

The parameters of the optimized peak filter is shown in TABLE III and TABLE IV.

The Bode diagram of the initial and optimized peak filter is shown in Fig. 5.

The sensitivity functions of the single-input single-output (SISO) open-loop system without the peak filter, with the initial peak filter, and with the optimized peak filter are shown in Fig. 6. It is shown that the optimized peak filter satisfied the constraints of the SISO sensitivity function.

$$\gamma - \left\| \mathrm{Re}\left(\frac{(\boldsymbol{D}^+_{(k_e,:)}(\mathrm{j}\omega_{k_f})(\boldsymbol{I}+\boldsymbol{G}(\mathrm{j}\omega_{k_f})\boldsymbol{F}(\mathrm{j}\omega_{k_f},\boldsymbol{\rho}_{(k_i-1)}))\boldsymbol{W})^*}{|\boldsymbol{D}^+_{(k_e,:)}(\mathrm{j}\omega_{k_f})(\boldsymbol{I}+\boldsymbol{G}(\mathrm{j}\omega_{k_f})\boldsymbol{F}(\mathrm{j}\omega_{k_f},\boldsymbol{\rho}_{(k_i-1)}))\boldsymbol{W}|}(\boldsymbol{D}^+_{(k_e,:)}(\mathrm{j}\omega_{k_f})(\boldsymbol{I}+\boldsymbol{G}(\mathrm{j}\omega_{k_f})\boldsymbol{F}(\mathrm{j}\omega_{k_f},\boldsymbol{\rho}_{k_i}))\boldsymbol{W}) \right) \right\|_1 \leq 0 \quad (23)$$

$$|w_{s,k_y}(\mathrm{j}\omega_{k_f})| - \mathrm{Re}\left(\frac{(G_{(k_y,k_y)}(\mathrm{j}\omega_{k_f})F_{k_y}(\mathrm{j}\omega_{k_f},\boldsymbol{\rho}_{(k_i-1)})+1)^*}{|G_{(k_y,k_y)}(\mathrm{j}\omega_{k_f})F_{k_y}(\mathrm{j}\omega_{k_f},\boldsymbol{\rho}_{(k_i-1)})|}(G_{(k_y,k_y)}(\mathrm{j}\omega_{k_f})F_{k_y}(\mathrm{j}\omega_{k_f},\boldsymbol{\rho}_{k_i})+1) \right) \leq 0 \quad (24)$$
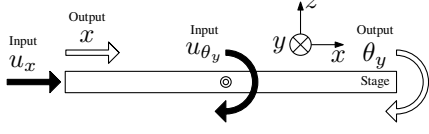
Fig. 2. 2-DOF motion system in translation x and pitching θ_y.
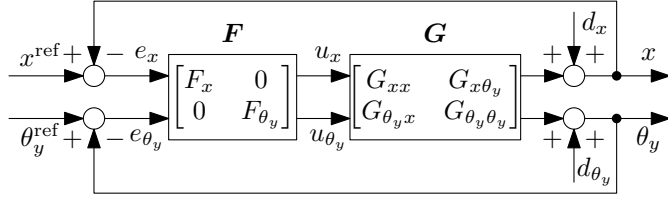
Fig. 3. Block diagram of 2-DOF given open-loop system $\boldsymbol{G}$ in translation x and pitching θ_y with designed diagonal peak filter $\boldsymbol{F}$.
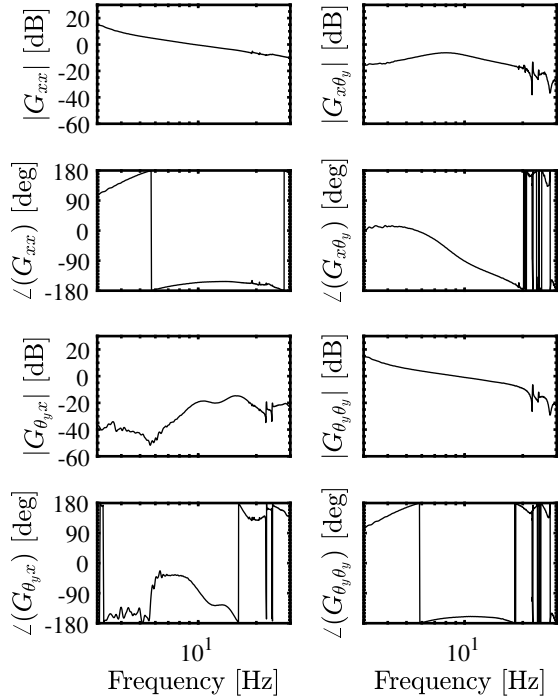
Fig. 4. Bode diagram of 2-DOF given open-loop system $\boldsymbol{G}$.

The Nyquist diagrams of the SISO open-loop system without the peak filter, with the initial peak filter, and with the optimized peak filter are shown in Fig. 7. It is shown that the SISO open-loop system with the optimized peak filter satisfied the Nyquist stability condition.

(a) x
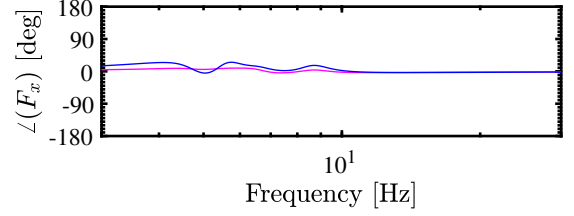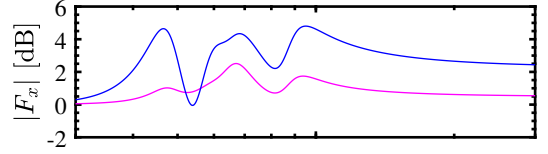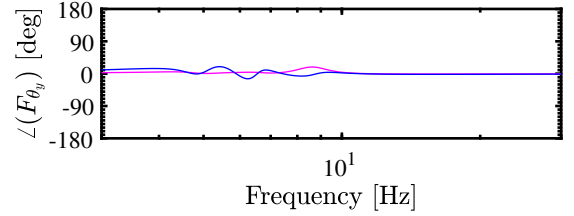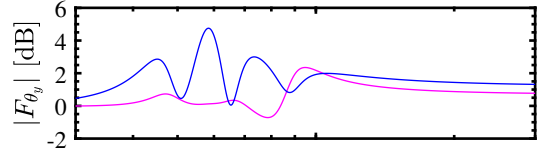
(b) θ_y

Fig. 5. Bode diagram of initial peak filter (——) and optimized peak filter (——).

D. Evaluation of disturbance rejection

The effectiveness of the optimized peak filter is evaluated in reducing the error.

The frequency response data of the error for the evaluation is given by the pre-experiment data in the worst case as follows:

$$\boldsymbol{e}_{\max}(\mathrm{j}\omega_{k_f}) = e_{\max,k_y}(\mathrm{j}\omega_{k_f}), \quad (29)$$

where $|e_{\max,k_y}(\mathrm{j}\omega_{k_f})| = \max_{\forall k_e} |e_{0,k_e,k_y}(\mathrm{j}\omega_{k_f})|$.

The frequency response data of the error with designed peak filter is calculated as follows:

$$\boldsymbol{e}(\mathrm{j}\omega_{k_f},\boldsymbol{\rho}) = \boldsymbol{S}(\mathrm{j}\omega_{k_f},\boldsymbol{\rho})\boldsymbol{S}_0^{-1}(\mathrm{j}\omega_{k_f})\boldsymbol{e}_{\max}(\mathrm{j}\omega_{k_f}). \quad (30)$$
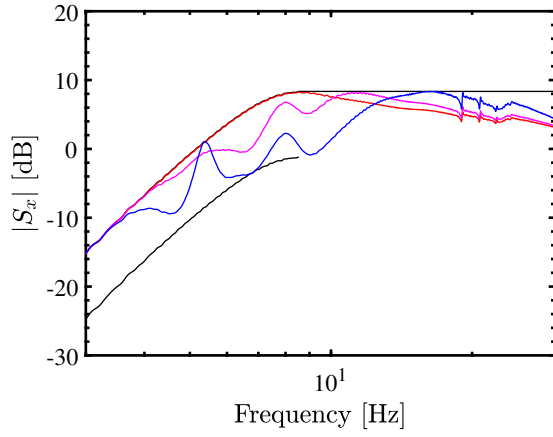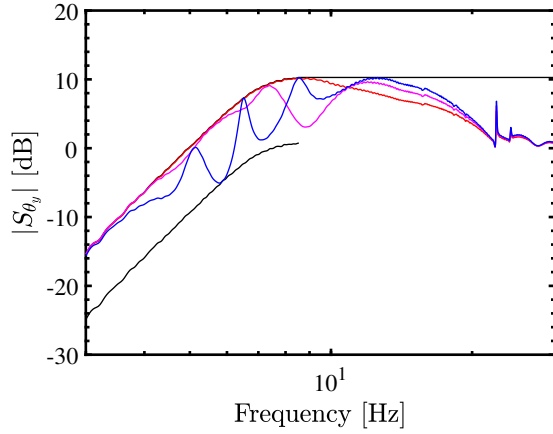
Fig. 6. Bode magnitude diagram of SISO sensitivity function without peak filter (——), with initial peak filter (——), and with optimized peak filter (——). Constraints of sensitivity function are shown in (——).

Fig. 7. Nyquist diagram without peak filter (——), with initial peak filter (——), and with optimized peak filter (——). Sensitivity peaks are shown in (——).

TABLE III
PARAMETERS OF OPTIMIZED PEAK FILTER F_x.

k_p	$\omega_{p,1,k_p}$	$\zeta_{p,1,k_p}$	$\rho_{1,k_p,1}$	$\rho_{1,k_p,2}$
1	$2\pi \times 4.78$	0.10	5.51	-6.02×10^{-02}
2	$2\pi \times 5.86$	0.10	3.36	1.39×10^{-01}
3	$2\pi \times 6.65$	0.10	1.74	9.72×10^{-02}
4	$2\pi \times 8.81$	0.10	0.66	1.25×10^{-01}

TABLE IV
PARAMETERS OF OPTIMIZED PEAK FILTER F_{θ_y}.

k_p	$\omega_{p,2,k_p}$	$\zeta_{p,2,k_p}$	$\rho_{2,k_p,1}$	$\rho_{2,k_p,2}$
1	$2\pi \times 4.78$	0.10	1.63	-1.14×10^{-01}
2	$2\pi \times 5.86$	0.10	11.64	4.07×10^{-02}
3	$2\pi \times 6.65$	0.10	-3.59	2.01×10^{-01}
4	$2\pi \times 8.81$	0.10	-3.02	2.37×10^{-02}

The amplitude spectrums of the error without the peak filter, with the initial peak filter, and with the optimized peak filter are shown in Fig. 8. It is shown that the maximum amplitude of the error is reduced by the optimized peak filter compared
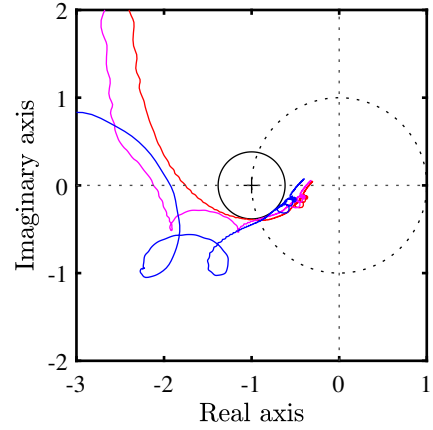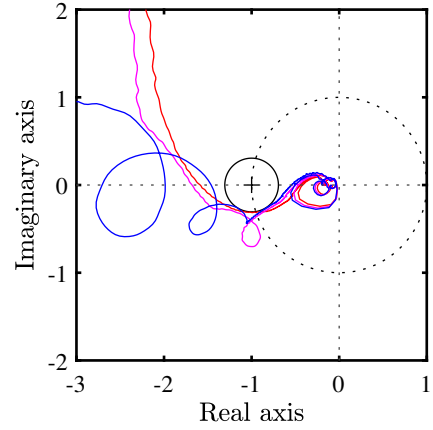
with other cases.

The cumulative amplitude spectrums of the error without the peak filter, with the initial peak filter, and with the optimized peak filter are shown in Fig. 9, where $f_{k_f} = 2\pi\omega_{k_f}$ and

$$E_{k_y}(f_{k_f}) = \sqrt{\frac{1}{2}\sum_{k_f}|e_{k_y}(j\omega_{k_f})|^2}. \tag{31}$$

It is noted that the final value of $E_{k_y}(f_{k_f})$ is equal to the root mean square of the inverse Fourier transform of $e_{k_y}(j\omega_{k_f})$. It is shown that the root mean square error is reduced by the optimized peak filter compared with other cases.

The results demonstrate the advantage of the proposed approach in the objective of minimizing the error.

V. CONCLUSION

The frequency response data-based multiple peak filter design is developed. The proposed approach improves the design method of the peak filter to reduce the error using convex optimization compared with other heuristic approaches. The
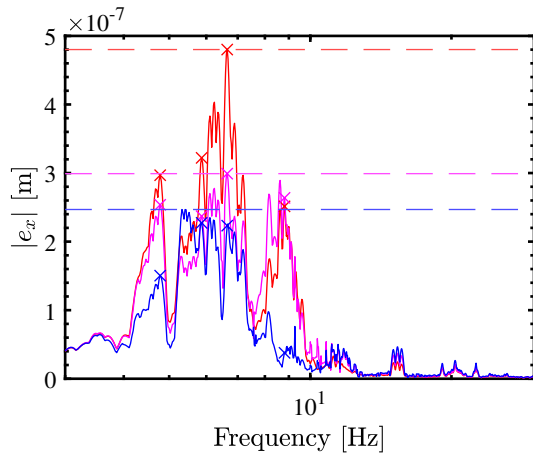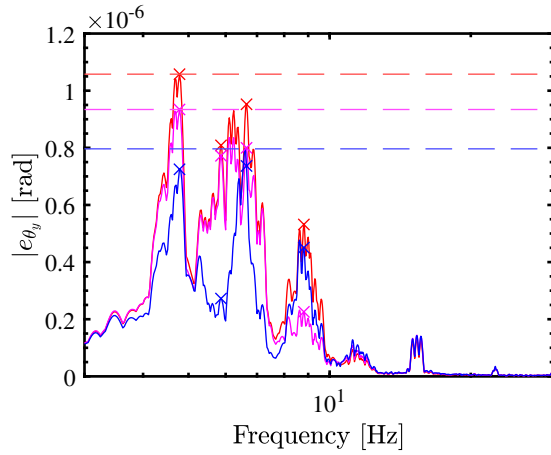
(a) x

(b) θ_y

Fig. 8. Amplitude spectrum of error without peak filter (——), with initial peak filter (——), and with optimized peak filter (——). Maximum amplitude is shown in horizontal dashed line. Peak filter is designed at peak error frequencies (×).
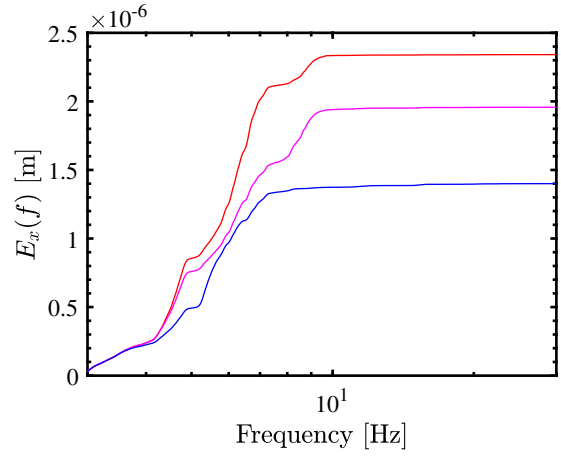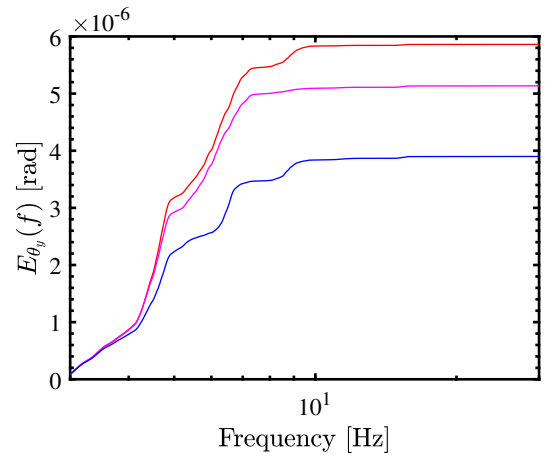

(a) x

(b) θ_y

Fig. 9. Cumulative amplitude spectrum of error without peak filter (——), with initial peak filter (——), and with optimized peak filter (——).

advantages of the approach are validated in the simulation with the 2-DOF motion system of a high-precision stage in the translation x and the pitching θ_y. Ongoing research focuses on application to the 6-DOF high-precision stage and experimental validation.

REFERENCES

[1] M. Steinbuch, T. Oomen, and H. Vermeulen, "Motion Control, Mechatronics Design, and Moore's Law," *IEEJ Journal of Industry Applications*, vol. 2, no. 4, p. 21006010, 2021. [Online]. Available: https://www.jstage.jst.go.jp/article/ieejjia/advpub/0/advpub_21006010/_article

[2] T. Oomen, "Advanced Motion Control for Precision Mechatronics: Control, Identification, and Learning of Complex Systems," *IEEJ Journal of Industry Applications*, vol. 7, no. 2, pp. 127–140, 2018. [Online]. Available: https://www.jstage.jst.go.jp/article/ieejjia/7/2/7_127/_article

[3] M. Mae, W. Ohnishi, H. Fujimoto, and Y. Hori, "Perfect Tracking Control Considering Generalized Controllability Indices and Application for High-Precision Stage in Translation and Pitching," *IEEJ Journal of Industry Applications*, vol. 8, no. 2, pp. 263–270, mar 2019. [Online]. Available: https://www.jstage.jst.go.jp/article/ieejjia/8/2/8_263/_article

[4] A. L. Yuille and A. Rangarajan, "The Concave-Convex Procedure," *Neural Computation*, vol. 15, no. 4, pp. 915–936, apr 2003. [Online]. Available: http://www.mitpressjournals.org/doi/10.1162/08997660360581958

[5] T. Atsumi, A. Okuyama, and M. Kobayashi, "Track-Following Control Using Resonant Filter in Hard Disk Drives," *IEEE/ASME Transactions on Mechatronics*, vol. 12, no. 4, pp. 472–479, aug 2007. [Online]. Available: http://ieeexplore.ieee.org/document/4282597/http://ieeexplore.ieee.org/document/4291569/

[6] B. A. Francis and W. M. Wonham, "The internal model principle for linear multivariable regulators," *Applied Mathematics & Optimization*, vol. 2, no. 2, pp. 170–194, jun 1975. [Online]. Available: http://link.springer.com/10.1007/BF01447855

[7] M. Mae, W. Ohnishi, H. Fujimoto, K. Sakata, and A. Hara, "Peak Filter Tuning based on Disturbance Spectrum for MIMO High-Precision Scan Stage," *IFAC-PapersOnLine*, vol. 53, no. 2, pp. 8413–8418, 2020. [Online]. Available: https://doi.org/10.1016/j.ifacol.2020.12.1577https://linkinghub.elsevier.com/retrieve/pii/S240589632032173X

[8] J. Lofberg, "YALMIP : a toolbox for modeling and optimization in MATLAB," in *2004 IEEE International Conference on Robotics and Automation (IEEE Cat. No.04CH37508)*. IEEE, 2004, pp. 284–289. [Online]. Available: http://ieeexplore.ieee.org/document/1393890/

[9] Mosek, "MOSEK 9.3," 2021. [Online]. Available: https://www.mosek.com